

Spatio-temporal behavior of a bistable optical system with global feedback

A.V. Larichev^a, F.T. Arecchi^{b,1}

^a International Laser Centre, Moscow State University, 199899 Moscow, Russian Federation

^b Istituto Nazionale di Ottica, 50125 Florence, Italy

Received 18 July 1994

Abstract

A bistable optical device, made of an extended system as a liquid crystal light valve (LCLV) plus a global feedback, displays a time dependent behavior whereby the fields corresponding to the two stable states fill different regions of the available space, and the boundary between the two regions moves periodically with a front velocity depending on the properties of the medium as well as on the feedback strength.

1. Introduction

Liquid crystals light valves (LCLV) have been introduced as noncoherent-to-coherent image converters for *passive* optical processing systems [1]. However, the high amplification of LCLV permits us to use a part of the output signal for feedback. The feedback not only improves the accuracy of analog optical processing systems [2] but also provides the possibility to create a spatially distributed *active* information system. The concept of *active* information system is based on the neural network approach to information processing [3,4]. One of the simplest types of the neural network is WTA (winner takes all), which is particularly interesting for pattern classifiers [5]. The global coupling between elements in the WTA network creates conditions such that eventually only one neuron with the largest input has non-zero output. LCLV based optical implementation of a neural network with WTA behavior has been suggested and theoretically investigated in Ref. [5].

Later, optical implementation of the WTA neural network based on a novel electron trapping material has been proposed [6], but so far it has not been completely realized experimentally.

Note that, in the LCLV based systems with optical feedback diffusion process in photoconductor and small misalignments in the optical feedback loop may lead to spatial instability [7]. This can create some difficulties in the experimental realization of the LCLV based WTA-type network. To eliminate this effect one can use a sampling light spot array [7]. Nevertheless, the spatio-temporal behavior of the dynamical system with global and local interactions remains a subject of interest.

In this paper we present the optical implementation of continuous WTA-type neural network. In order to realize a global coupling we use the dependence of the LCLV spatial uniform phase shift on the amplitude of applied voltage. This solution effectively simplifies optical and electronical parts of setup. We report a regime in which different fixed points of the dynamical system are stabilized in different spatial regions, as well as a time dependent regime in

¹ Also Phys. Dept., University of Florence, Florence, Italy.

$$V_{PS} = V_{PS}^0 + B + \alpha \int_S I(\mathbf{r}, t) \, d\mathbf{r}, \quad (4)$$

where V_{PS}^0 is the initial voltage of PS. By changing this voltage we can choose the initial phase shift φ_0 (in our experiments $\varphi_0=0$).

A noncoherent light source LS with condenser CD is used for illumination of the amplitude slide SL. The image of SL is formed by lens L_6 on the input end of the fiber bundle F. This scheme permits to produce an additional spatial non-uniform phase shift $u_0(\mathbf{r})$. By substituting expressions (2)–(4) into (1) and using a linear approximation for the function f one can obtain the complete equation for the nonlinear phase modulation $u(\mathbf{r}, t)$

$$\tau \frac{\partial u}{\partial t} + u = l^2 \Delta_{\perp} u + K \left(1 + \cos u + B - \alpha \int_S (1 + \cos u) \, d\mathbf{r} \right) + u_0(\mathbf{r}), \quad (5)$$

where K is the amplification factor of feedback. This model is identical with the model of continuous WTA neural network, which was numerically investigated in Ref. [5].

3. Experimental demonstration of extrema selection

In order to show the possibility of the 2D function's extrema selection we install at the input plane of the illumination system a slide with the following transmission distribution

$$T(\rho, \varphi) = \sin^2(2\varphi) \sin^2(\sqrt{2\rho} + \pi/2), \quad (6)$$

where ρ, φ are the polar coordinates at the input plane. This function has four maxima with equal amplitude. In this experiment B and α are close to unity. Fig. 2a shows the output intensity distribution with closed optical feedback (without electronic feedback). Since the optical feedback automatically adjusts the working point of LCLV in inversion contrast mode, the minima on Fig. 2a correspond to maxima of $T(\rho, \varphi)$. Nonlinearity and spatial inhomogeneities in LCLV induce distortions of maximum amplitudes. As result we have four minima with different amplitudes. The output intensity distribu-



Fig. 2. Examples of extrema selection: (a) optical feedback ON, electronic one OFF, (b) optical and electronic feedbacks both ON.

tion with closed optical and electronic feedbacks is shown on Fig. 2b. Two bright spots appear at the location of lower level minima. Size and shape of these spots are determined by the concavity close to the minima. The integrated intensity on the feedback loop, and consequently the total area of bright domains, is controlled via B and α . The output intensity distribution with small bright spots, however, is unstable. Under small perturbations of the laser or of the noncoherent illumination source, bright spots disappear.

The transition process from the only optical feed-

back (Fig. 2a) to the optical and electronic feedbacks (Fig. 2b) is characterised by two different stages. The first stage corresponds to the formation of the output intensity distribution of the type “bright spots on dark background”. The shape and location of spots roughly agree with the form and position of the initial intensity distribution minima. The duration of this stage is approximately $2-3\tau$. In the second stage the system more precisely adjusts the shape and location of the bright domains. This stage lasts as long as the velocity of the domain boundaries is non-zero. Its duration is more than 10 times longer than that of the first stage. The characteristic time of the second stage is determined by the velocity of switching waves and consequently by spatial resolution (i.e., diffusion length l) and response time τ of LCLV.

Increase of α leads to reduction of bright domain's area and total transition time. However, when α becomes higher than 1.2–1.4, spatio-temporal oscillations appear.

4. Spatio-temporal self-oscillations

Since the oscillation behaviour of the system with additional non-coherent illumination is rather complicated, we restrict our attention to the case without it. In this condition, the initial (with optical and electronic feedback OFF) output intensity distribution has some modulation along the x axis (shown in Fig. 3c). This modulation corresponds to initial linear phase modulation in LCLV. The amplitude of this phase modulation is approximately $\pi/6$. When optical and electronic feedbacks are ON and α is sufficiently large, spatio-temporal oscillations are excited. Fig. 3 illustrates the main stages of this process. The bright domain arises close to the minimum of the initial intensity distribution. The intensity and size of this domain and also the intensity of dark background change in time (compare Fig. 3a and Fig. 3c). The dark and bright boundary layers are observable on Fig. 3b and Fig. 3e, respectively.

The time dependence of the intensity over a beam cross-section (space-time plot) is reported in Fig. 4a. This space-time plot is obtained experimentally by stroboscopic recording of 48 intensity distributions with the same system parameters as in Fig. 3. The dashed line on Fig. 3c indicates the position of the

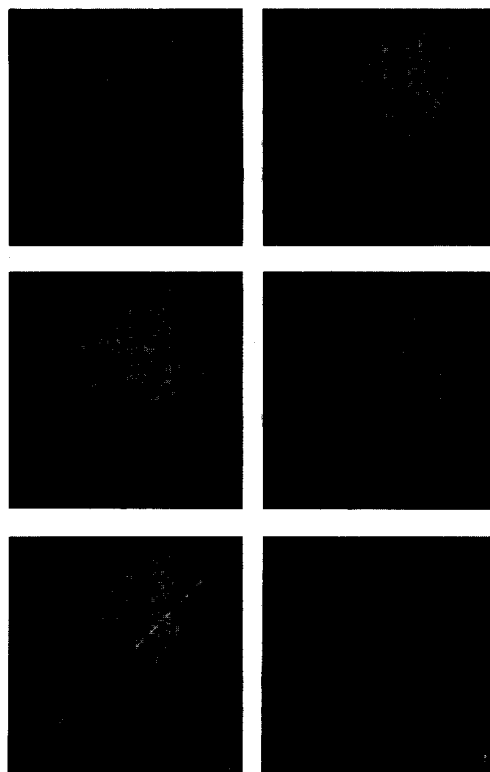


Fig. 3. The main stages of spatio-temporal oscillations ($\alpha = 1.9$; $b = 0.6$).

cross-section. From Fig. 4b one can obtain information about the time behaviour of intensity I_b within the bright domain and I_d within the background. The time dependence of the total size \bar{S}_b of the bright domain and its approximation by a cosine function are also given in Fig. 4b. Here we use the normalized size $\bar{S}_b = (S_b - S_b^{\min}) / S_b^{\max}$, where S_b^{\min} , S_b^{\max} are minimum and maximum sizes of the bright domain. It is easy to see that intensities I_b and I_d oscillate with the same phase. The oscillation of the bright domain total area, however, has a phase shift $\Delta\phi$ in the range $3\pi/4 < \Delta\phi < \pi$ with respect to these intensities. It corresponds to the fact that variations of \bar{S}_b are caused by switching processes in the boundary layer of the bright domain. The characteristic time of these processes depends not only on the LCLV response time τ and optical feedback gain K , but also on the LCLV spatial resolution. As result the equivalent response

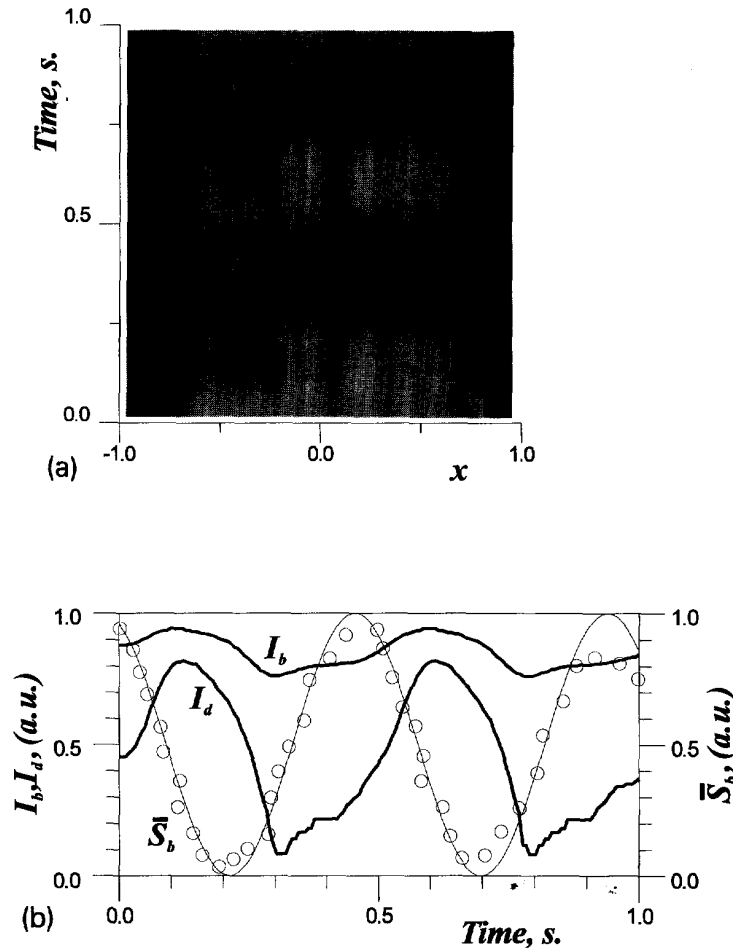


Fig. 4. Time behavior of output intensity in the 1D cross-section of the beam: (a) space–time plot, (b) time dependences of I_b , I_d and \bar{S}_b .

time for bright domain size variations is higher than the response time for I_b and I_d .

In analogy with biological and chemical systems, we consider our system as a dissipative two-component nonlinear system [10]. The intensities I_b , or I_d , play the role of the first component, since they have a similar time behavior. The bright domain size \bar{S}_b can be selected as the second component. For particular sets of feedback gains K and α the cosine nonlinearity can be approximated by a N -type curve, that is generic for many chemical and biological systems. In view of these facts, it is possible to explain the existence of self-oscillations regimes in the system.

However, it is well to bear in mind that this anal-

ogy is fairly rough and can explain only the simplest features of the system dynamics. More complex regimes are excited in the area of multistability of the system, which is connected with the cosine-type nonlinearity.

Sets of experiments have been carried out for studying the influence of α on the behavior of the system. Typical results are presented in Fig. 5. Figs. 5a, 5c and 5e show phase trajectories for time series of the integrated feedback intensity

$$I_f = \int_s 1 + \cos(u + \varphi_0) dr.$$

Figs. 5b, 5d and 5f show the power spectra of these

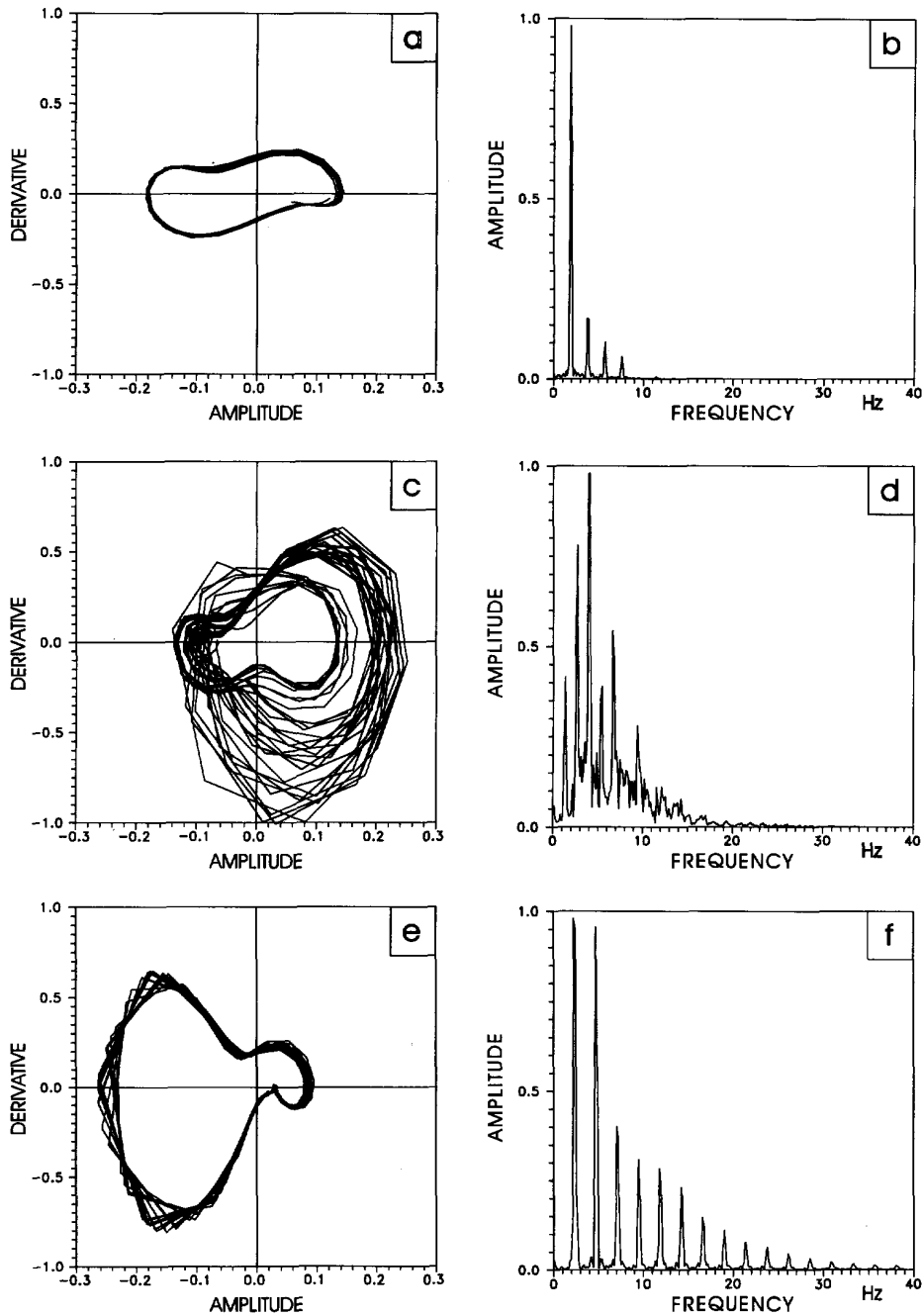


Fig. 5. Phase trajectories (a, c, e) and spectra (b, d, f) of output integrated intensity. ($K=8$; $B=0.6$), (a, b) $\alpha=1.9$, (c, d) $\alpha=2.7$, (e, f) $\alpha=3.0$.

time series. Near the excitation threshold the form of oscillations is close to a harmonic function (Fig. 5a, b). Increasing α adds complexity to the oscillations. At the $\alpha=2.7$ the spectrum (Fig. 5c) contains several frequencies over a continuous background. This type of spectrum and the associated phase trajectories (Fig. 5d) suggest that a strange attractor is present. The further increases of α leads again to periodic motion (Fig. 5f).

The minimal model to describe the limit cycle behavior is made of the following elements. In the uniformly bright or dark regions the reaction-diffusion equation (5) for u can be approximated as a diffusionless equation for a space independent u -field

$$\tau \frac{du}{dt} + u = F(u) - \alpha z. \quad (7)$$

Here $F(u) = K(1 + \cos u)$ represents the optical feedback, while the variable z is the integrated intensity providing the global electronic feedback. It can be expressed in term of the localized position ($0 < x < 1$ in normalized units) of the boundary front between the first and second solution of the bistable stationary equation emerging from Eq. (7), that is,

$$u + \alpha z = F(u). \quad (8)$$

We schematize the model for the one dimensional case (justified if the two domains are separated by a regular boundary as in Fig. 3). We approximate the working range of $F(u)$ (i.e., the range around the intersection with the linear function $u + \alpha z$ as in Eq. (8)) by a cubic, which provides three solutions for Eq. (8): u_1, u_3 are stable and the intermediate one u_2 is unstable.

The velocity of the switching front x between the two stable solutions is uniquely specified in terms of the solutions of Eq. (8) as (see Ref. [12], Eq. (11.07))

$$dx/dt = \beta(u_1 - 2u_2 + u_3), \quad (9)$$

where β is a suitable combination of parameters of the model.

Eqs. (7)–(9) must be completed by a functional relation $z(x)$ for the integrated intensity in terms of the front position. For instance, in the drastic approximation of the cubic as three pieces of straight line, two vertical ones located at $u_1=0$ and $u_3=\pi$ and a connecting third piece of slope 2α , the relation $z(x)$ is simply

$$z(x) = x, \quad (10)$$

since we must weight the two intensities $I_b = \frac{1}{2}(1 + \cos u_1) = 1$ and $I_d = \frac{1}{2}(1 + \cos u_3) = 0$ with x and $1-x$, respectively. Similarly in this case Eq. (9) becomes

$$dx/dt = \beta(1 - 2\alpha x). \quad (11)$$

Numerical solutions of Eq. (7) coupled to Eq. (11) provide very easily limit cycle behavior. Even without these drastic approximations, the single species model of Eq. (7) coupled via $z(x)$ to front velocity of Eq. (9) gives limit cycle oscillations which mimic what observed experimentally in Fig. 5. The more realistic $F(u) = K(1 + \cos u)$ provides more than three solutions of Eq. (8) and this makes possible a chaotic behavior. A more detailed analysis will be presented elsewhere.

5. Conclusions

The extremum selection in the input image by a nonlinear optical system with WTA-type dynamics has been demonstrated. Diffusive coupling limits the accuracy of selection and decreases its speed. The radical solution of this problem is presumably possible by using a specific LCLV with internal mirror consisting of separated subapertures. This proposal is basically the same as sampling of input beam [7], but it seems more convenient for our optical scheme. Furthermore, the simultaneous coexistence of different solutions in separate space regions has been experimentally demonstrated, and the boundary between the two regions was shown to undergo periodic or chaotic motion. A simple model captures the essence of this dynamic behavior.

Acknowledgements

We acknowledge M. Vorontsov, who has initiated this work. The useful discussions and assistance in experiments of P.L. Ramazza and S. Residori are appreciated. This work has been partially supported by EEC-Esprit Basic Research action TONICS.

References

- [1] W.P. Bleha, L.P. Lipton et al., *Opt. Eng.* 17 (1978) 371.
- [2] M.A. Vorontsov, *Proc. SPIE* 1402 (1991) 116.
- [3] R.C. Lippmann, *IEEE Communication Magazine* (November, 1989) 47.
- [4] T. Kohonen, *Self-organization and associative memory* (Springer, Berlin, 1988).
- [5] E.F. Kobzev and M.A. Vorontsov, *Proc. SPIE* 1402 (1991) 137.
- [6] Xiangyang Yang, W. Seiderman, R.A. Athale, M. Astor and N.P. Cavaris, *Optics Comm.* 93 (1992) 33.
- [7] Yong Qiao and D. Psaltis, *Optics Lett.* 17 (1992) 1376.
- [8] H. Gibbs, *Optical Bistability: Controlling Light with Light* (Academic, London, 1985).
- [9] S.A. Akhmanov, M.A. Vorontsov, V.Yu. Ivanov, A.V. Larichev and N.I. Zheleznykh, *J. Opt. Soc. Am. B* 9 (1992) 78.
- [10] J.D. Murray, *Mathematical Biology* (Springer, Berlin, 1989).